NASA GRANT
NGR-33-008-146

THEORY OF TIME-DEPENDENT RUPTURE IN THE EARTH[1]

S. Das and C. H. Scholz[2]

Lamont-Doherty Geological Observatory of Columbia University

Palisades, New York 10964

ABSTRACT

Using the concepts of fracture mechanics, we develop a theory of the earthquake mechanism which includes the phenomenon of subcritical crack growth. The theory specifically predicts the following phenomena: slow earthquakes, multiple events, delayed multiple events (doublets), postseismic rupture growth and afterslip, foreshocks, and aftershocks. The theory also predicts that there must be a nucleation stage prior to an earthquake, and suggests a physical mechanism by which one earthquake may 'trigger' another.

These predictions are obtained by combining two fundamental concepts. The first is that

$$k = C\,\Delta\tau\sqrt{X}$$

and the second, that

$$k = K_o \left(\frac{\dot{X}}{V_o}\right)^{1/n}$$

where k is the stress intensity factor, $\Delta\tau$ stress drop, X rupture length, $\dot{X}$ rupture velocity, C a geometrical factor, and K_o, V_o, and n are material constants. The first is a fundamental result of fracture mechanics; the second describes stress

[1]Lamont-Doherty Geological Observatory Contribution No. 0000.

[2]Also at: Department of Geological Sciences, Columbia University.

corrosion cracking, a well established physical process that results in subcritical crack growth.

We investigate in detail two phenomena of special interest and which are not predicted by ordinary fracture mechanics: nucleation and delayed multiple events. In the first case we find that all earthquakes must be preceded by quasistatic slip over a portion of their rupture surfaces, but it may be difficult to detect in practice. In the second case we studied two pairs of delayed multiple events that were separated by the same 'barrier' in order to calculate n. We find that the stress corrosion index, $n \sim 24$.

GLOSSARY OF SYMBOLS

C = geometric constant = 1 for a two-dimensional crack
= $20/7\pi\sqrt{2}$ for a circular shear crack

k = stress intensity factor

k_D = dynamic stress intensity factor

k_s = static stress intensity factor

K_o = stress corrosion limit

K_c = modulus of cohesion in the presence of corrodent

K^*_c = modulus of cohesion under corrodent-free conditions

K_1 = a fixed arbitrary point on the $(k\text{-}\dot{X})$ curve

L = barrier width

ℓ_1, ℓ_2 = lengths of rupture zones of two events in a pair of delayed multiple events

m = frequency of aftershock occurrence

n = stress corrosion index

t = time since occurrence of main shock

t_D = delay time between a pair of multiple events

t_R = maximum of rise times of individual events in a sequence of multiple events

t_f = time to failure (instability) or nucleation time of an earthquake

t' = $t - \Delta t$

u = slip on crack plane

V_o = crack growth velocity at the stress corrosion limit

V_1 = X - coordinate corresponding to K_1

W_o = a material property

X = crack length (for two-dimensional cracks) and crack radius (for circular shear crack)

$\dot{X}$ = crack edge velocity

X_o = initial X

X_f = X at time t before failure

β = an elastic wave velocity

$\Delta\tau$ = static stress-drop

Δt = short time before instability

INTRODUCTION

In recent years the developments of linear elastic fracture mechanics have been applied to an important problem in geophysics: development of a dynamic model of earthquakes [Kostrov, 1966; Richards, 1976; Andrews, 1976; Fossum and Freund, 1975; Das and Aki, 1977a,b; Freund, 1979]. The central concept of fracture mechanics, which has its roots in the Griffith energy balance [Lawn and Wilshaw, 1975], is that for a crack in an elastic medium, no propagation takes place until the stress intensity factor at the crack tip, k, reaches a value K_c, a property of the medium. K_c is called the "modulus of cohesion" [Kostrov et al., 1969]. When $k \geq K_c$, the Griffith instability arises and the crack propagates dynamically with a velocity limited by an elastic wave velocity.

Most oxides and silicates, however, exhibit more complicated behavior due to environmental effects. For these materials, the crack will propagate when $k \geq K_o$, where $K_o < K_c$, at a velocity $\dot{X}$ which is a well defined function of k. This propagation is stable and quasistatic and is referred to as subcritical crack growth. (We shall use the terms "stable", "quasi-static" and "subcritical" to mean propagation at velocities much less than the sonic velocities of the medium). This behavior results from stress induced corrosion at the crack tip, the principal corrodent for the present application being H_2O. This behavior has been firmly established in the laboratory for Mode I (tensile) cracks in a wide variety of materials including silicates and silicate glasses [see, e.g., Scholz, 1968a, 1972a; Martin, 1972; Wiederhorn and Bolz, 1970; Atkinson, 1979; Lawn and Wilshaw, 1975; Knott, 1973].

The form of the relationship between k and $\dot{X}$ does not vary significantly with the material; only the parameters in the law vary. As an example we show in

Figure 1 data on subcritical crack growth in quartz [after Atkinson, 1979]. The empirical relationship is found to take the form,

$$\dot{X} \propto k^n \tag{1}$$

or

$$\dot{X} \propto e^k \tag{2}$$

Since n, the stress corrosion index, is large (12.5 in Fig. 1), 1 and 2 are nearly indistinguishable.

Since a shallow focus earthquake is a shear crack growing in silicate in an aqueous environment, eqn. 1 or 2 should be used as a complete description of the fracture process. Since an earthquake is a mixed Mode II and III shear crack and data are only available for the Mode I case, this involves an assumption: that the form of the law (but not necessarily the parameters) does not depend on mode (Atkinson's method may actually put the crack into mixed Mode I and III, an unsupported statement in Evans [1972] being the only argument to the contrary). Later we shall determine n for an earthquake and show that it is in remarkable agreement with Atkinson's results. Although we cannot prove this assumption, it seems entirely reasonable since when one considers the physical mechanism of stress corrosion there seems to be no physico-chemical reason why the process should depend on mode. The indirect evidence in support of this is that rock exhibits dilatant creep and static fatigue, both processes that result from stress corrosion, in compression and under high confining pressure [Scholz, 1968a; Kranz and Scholz, 1977; Kranz, 1980]. We shall also assume that there is a lower limit, K_o, such that when $k < K_o$ no crack growth occurs. There is only limited data to

support this [Wiederhorn and Bolz, 1970; Evans, 1972] but it is well founded in stress corrosion theory. In any case, our results are not critically dependent upon this assumption of a stress corrosion limit, because if it does not exist, we can simply define K_0 as a value of k below which the crack velocity is vanishingly small and can be neglected.

It should also be pointed out that in using eqns. (1) or (2) and the fracture mechanics approach, we are implicitly assuming that the most important forces governing the propagation of the rupture are the forces at the crack tip and that the friction that acts on the crack behind the crack tip plays no role on the motion of the crack tip. This is clearly an approximation, but the complete problem cannot be handled until the full energy balance, as discussed by Kostrov [1974] can be solved. For the present time, we will have to justify this assumption with the success we have, with our present approach, in predicting the observations.

In this paper, then, we consider an earthquake as a shear crack that propagates according to a law given by (1) up to the time when the propagation becomes dynamic. This theory predicts a variety of phenomena, all of which have been observed for earthquakes. The phenomena which arise quite naturally in the theory are slow earthquakes, multiple events, delayed multiple events (doublets), aftershocks, foreshocks and postseismic rupture extension and afterslip. The model also contains specific predictions about the earthquake nucleation process. All of these phenomena we now see simply as different facets of the same phenomenon.

In order to underscore the underlying simplicity of this model, we will first qualitatively describe how the various phenomena noted above arise, and then follow that with a quantitative model which we will apply to several examples.

IMPLICATIONS OF THE THEORY

For a crack in an infinite, homogeneous, elastic medium, the relationship between crack length, X, and stress intensity factor, k, at the crack tip is

$$k \propto \sqrt{X} \tag{3}$$

regardless of mode. If $k \geq K_o$ we immediately see, combining (3) with (1) that the crack will accelerate to a catastrophe (this is a stronger catastrophe than a Malthusian one since the latter is a simple exponential), the relevant equations for which are given in a later section. This catastrophe occurs when the crack becomes critical and propagates dynamically. We shall show later that this occurs at a well defined value of k, which we will call K_c. Note that K_c is different from K^*_c, the value of k at which instability occurs in the absence of stress corrosion. K^*_c is a material property that for these materials can be measured only in a corrodent-free environment, e.g., a high vacuum. K_c, on the other hand, is not an independent material property, it depends on n. We do not assume a value of K^*_c in our problem, we calculate a value of K_c. If $K_c \leq K^*_c$, then we need not consider K^*_c at all. If $K^*_c < K_c$ then the instability will occur earlier than we calculate, but otherwise our results will be unchanged. It is most likely, in fact, that $K_c = K^*_c$, since as the crack-edge velocity approaches sonic velocities, the crack is propagating too fast for the corrodent to diffuse to the crack-edge and a vacuum exists at the tip of the crack [Wiederhorn, 1967]. It may not seem obvious at first that this will occur for a shear crack, but for a topographically rough surface it is unlikely that shear can take place without some dilation. The velocity, V_o, at K_o is also important and will be discussed in a later section.

The stress intensity factor in (3) is simply the applied stress at infinity (or in the case of a crack with friction, the stress drop) multiplied by some geometrical factors. On the other hand, the fracture criterion (1) depends on the material properties K_o and n. Since a fault is not a homogeneous surface, both the applied stress and hence k, and the material properties K_o and n will be functions of position on the fault plane. Since a fault plane consists of two surfaces in contact, and the topography of surfaces is known to be Brownian [Sayles and Thomas, 1978] or fractally Brownian [Mandelbrot, 1977], we should expect that the heterogeneity of applied stresses and material properties is at least as random as the topography and that this heterogeneity exist at all scales. If we compare a fault plane with a mathematically flat plane, it is one of the properties of Brownian surfaces that the standard deviation from a flat plane increases as $x^{1/2}$, where x is a scale length of the section of the Brownian surface that is sampled. We should therefore consider K, n, and K_o as random variables on the fault plane and the rupture process a stochastic growth process [see, also, the discussion in Scholz, 1968b]. Then the sampling dimension x becomes the earthquake radius or length dimension, and the consequence of the fault being a Brownian surface is that the larger the earthquake becomes, the larger will be the wavelength and intensity of heterogeneities that it encounters. The only reason smaller earthquakes appear simpler than larger ones is due to the fact that we observe earthquakes with band-limited instruments and because the higher frequency waves radiated by the smaller heterogeneities are more strongly attenuated in propagating from the source to the instrument.

For the purpose of the remainder of this discussion, however, we will consider only gross heterogeneities which we will call barriers, after the usage of Das and Aki [1977b]. These are regions on the fault plane that are particularly resistant to slip either because of low applied stress or exceptionally high strength properties. The term barrier, then, refers to a heterogeneity of sufficient size that its effects on the rupture propagation can be observed instrumentally.

We are now ready to discuss the broader implications of the model. We will do so by discussing as scenarios the various possible phenomena that can result due to spatial and temporal variations in k, K_o, and n on the fault. These scenarios are illustrated in Figures 2 and 3.

Nucleation. The loading that is implied in the elastic rebound theory [Reid, 1910] is a tectonic process consisting of a steady increase in the applied stress, at a very slow rate, such stress being released by the earthquake. This tectonic loading process is equivalent to a steady increase in k for a potentially growing crack. It is usually thought that no motion occurs until $k = K_c$, when the earthquake initiates. With a fracture process such as described by (1), however, this is impossible. Instead, propagation of the crack begins when $k = K_o$, and it quasistatically accelerates up to sonic velocity at $k = K_c$ (Figure 2). It is thus fundamental to this model that an earthquake be preceded by some precursory slip. We call this stage the nucleation phase. The size of the nucleation region and the time scale of the process depend only on n and K_o and their spatial distributions on the fault. Because of its importance to earthquake prediction, we will discuss this quantitatively later. See Smith and Wyss [1968], Sacks [1978], Sacks et al. [1980, 1981], and Kanamori and Cipar [1974] for possible observational examples.

Slow earthquakes. Although the catastrophe implicit in (3) and (1) is very strong, there is a finite probability, because of the heterogeneity of the fault, that the rupture will propagate into regions in which $k < K_o$ during the nucleation phase and stop. What results is a slow earthquake [Kanamori, 1972; Kanamori and Stewart, 1979; Sacks et al., 1978]. We expect, of course, that this is an uncommon phenomenon but worthy of study because it yields a minimum estimate of the moment in the nucleation phase.

Foreshocks. During the nucleation phase, we can also expect it to be likely that $k \geq K_c$ for small regions of the fault within the nucleation region. These

regions will grow dynamically, only to stop by running into adjoining regions where $k < K_c$. When this happens, a foreshock results. Because of the accelerating nature of the nucleation process, the probability for foreshocks to occur increases very rapidly as the time approaches the time of the main shock. Note also that foreshocks are not an intrinsic part of the nucleation process so that they are not required to fit any regular pattern nor are all earthquakes required to have foreshocks. All three of these predicted properties of foreshocks mentioned above are confirmed in the observations. This suggests that the study of foreshocks may provide information concerning the spatial and temporal development of the nucleation phase.

Stopping. In nucleation, only two possibilities can occur: a slow earthquake or a 'normal' earthquake (Figure 2). In the stopping process, however, more possibilities can occur (Figure 3). When a rupture is propagating dynamically, the stress-intensity factor at its tip is a dynamic one, k_D. (All k's up to now were static stress-intensity factors.) The rupture will stop propagating at a point on its perimeter when $k_D < K_c$, but slip will continue within the rupture perimeter as the displacement field tends to static equilibrium. After static equilibrium has been reached there will be a static stress-intensity factor k_s at the crack tip, where $k_s > k_D$ [see Achenbach, 1973, eqn. 5.7]. It is this extra complication that produces the additional phenomena.

For simplicity we will assume that the rupture stops at a barrier where $k_D < K_c$ (a barrier is indicated by a sawtooth in Figure 3). What happens next depends on the properties of the barrier. If:

$k_s < K_o$. The trivial case results. The earthquake simply stops and the barrier becomes the end of the rupture (Figure 3a).

$k_s \geq K_c > k_D$, the barrier is breached before slip stops within the perimeter and a multiple event occurs, with a delay time $t_D \leq t_R$, the rise time

(Figure 3b). By rise time we mean the average slipping time within the rupture. This is the type of multiple event first described by Wyss and Brune [1968] and modelled by Das and Aki [1977b]. It is worth remarking that because heterogeneity exists at all scales, earthquakes are by their very nature infinitely multiple. It is simply that our data allow us to describe only the gross heterogeneities.

$K_o < k_s < K_c$. This is an interesting case because, unlike those discussed above, it cannot be explained on the basis of ordinary fracture mechanics. In this case the rupture subcritically propagates through the barrier, going critical when it breaches the barrier after a time delay $t_D >> t_R$. This results in an earthquake occurring just adjacent to a previous earthquake and a short time after it. We call this process a delayed multiple event (Figure 3c). That this type of event occurs has been very well documented for the Nankai trough of western Japan by Ando [1975]. The most prominent events discussed there are the Ansei I and II (1854) events, adjacent earthquakes with a time delay of 32 hours, and the Tonankai (1944) and Nankaido (1946) events, separated by two years. We shall model these two pairs below, and calculate n and K_o from then. This type of multiple event is common in some regions [Sykes, 1971; McCann, 1980; Lay and Kanamori, 1980].

There are two differences between these two types of multiple events. The first is the delay time, the other is more subtle. Denote by ℓ_1 the length of the rupture just as the barrier is encountered, and ℓ_2 as the distance the rupture propagates after breaching the barrier. In the ordinary multiple event, the region ℓ_1 has not come to static equilibrium when the barrier breaks, so that the region in ℓ_1 continues to slip as the rupture propagates to its final dimension $\ell_1 + \ell_2$, and the source parameters are those of a single earthquake of rupture dimension $\ell_1 + \ell_2$. In the case of the delayed multiple event, however, the region ℓ_1 comes to static equilibrium before the barrier is breached and the static frictional

strength is re-established, and increases with time of static contact [Scholz and Engelder, 1976; Dieterich, 1978]. In this case, when the barrier is breached, only the new region ℓ_2 slips, and the result is two earthquakes with source parameters appropriate for rupture dimensions ℓ_1 and ℓ_2, respectively.

It is of course not necessary that the barrier be breached in this case. If the barrier were to, say, increase in strength with distance faster than $\sqrt{x}$, the rupture may grow into the barrier for some distance and then stop, when $k < K_0$, as in Figure 3d. If this occurs we will observe postseismic rupture growth. A number of cases of this have been documented, the most prominent being the 1946 Nankaido earthquake [Ando, 1975], in which half the rupture area failed quasistatically. (It is interesting that the region that ruptured quasistatically also had no aftershocks. Our model would predict fewer aftershocks, but not a complete absence of aftershocks. The data should be re-examined to specifically address this question.) If the original rupture area slips quasistatically as the rupture grows quasistatically, we would observe afterslip. This appears to be a fairly common phenomenon, but of secondary importance, since it normally contains less than 5% of the moment of the main shock [Scholz, 1972b]. Indeed, the Nankaido case is probably an exceptional one, because rupture zones of large earthquakes are commonly observed to nearly abut [Sykes, 1971]. Thus postseismic rupture growth usually appears not to extend the rupture more than a small percentage of its original length, though exceptional cases may occur and thus be of interest to those who study seismic gaps.

Aftershocks. Slip of a heterogeneous fault during an earthquake will only on average tend to the static slip distribution expected for the homogeneous case. On a local scale, small patches may slip less (or more) than surrounding regions and thus be dynamically loaded, rather than unloaded, during the earthquake. Note that the barrier of Das and Aki [1977b] is an extreme case of these patches, i.e.,

one that does not slip at all. Since the earthquake occurs dynamically, this loading is very rapid, and the k for these regions can take any value $k < K_c$. Thus the initial conditions are set at the time of the main shock. Any patch for which $K_o < k < K_c$ will grow quasistatically to failure with a time delay that can be calculated from (1) (see Figure 3e). Thus aftershocks are predicted by the model, and should have the following characteristics:

a. Since large earthquakes can be expected to be heterogeneous, the occurrence of aftershocks, unlike foreshocks, should be nearly ubiquitous.

b. Aftershocks should be distributed all over the plane of rupture, not necessarily uniformly, and it is likely that a concentration of them will occur near the ends of the rupture, where the large scale stress concentration exists.

c. If k is distributed randomly between K_o and K_c for the population of patches, then the frequency of failure of these regions, m, will be a function of time, t, after the main shock and will take the form,

$$m \propto \frac{1}{t} \tag{4}$$

The derivation of (4) is given in Scholz [1968b] and follows from a static fatigue law of the type found by Mould and Southwick [1959]. This law was shown to be derivable from eqns. 1 or 2, by Wiederhorn and Bolz [1970].

d. Aftershocks are a second order effect relative to the main shock since they result only from deviations from the mean, so the sum of their moments should be only a small fraction of the moment of the main shock. This is one way to distinguish them from delayed multiple events.

One other property of aftershocks which is not directly implied by the model but seems likely is that aftershocks within the perimeter of the rupture zone will statistically tend to occur in isolated patches and hence these aftershocks will not

tend to have aftershock sequences of their own. Aftershocks that occur on the perimeter, and which therefore extend the perimeter, may, on the other hand, produce aftershocks. This effect was observed by Page [1968] for the 1964 Alaska earthquake.

The properties of aftershocks are sufficiently well known that it is not necessary to cite particular examples to state that the observations bear out the above predictions of the model. The prediction of the Omori Law (eqn. 4) is particularly important. In order to see how consistently aftershock sequences obey this law and the other above predictions, one should consult the compendia of Utsu [1969, 1970, 1971, 1972].

Deep earthquakes. In the above discussions we have tacitly been concerned only with tectonic earthquakes of shallow focus, as defined in the usual way. Deep focus earthquakes, on the other hand, do not conform to some of the predictions of the model. Most prominently, they do not have aftershock sequences. This may result either because the corrodent responsible for this behavior, free H_2O, is not present at those depths or simply because the mechanism of deep earthquakes is not the type of rupture process that we are discussing.

In the above we have taken a time dependent fracture criterion, which is well established experimentally, and applied it to the earthquake process. Since we know that $K_c > K_o$ always, $k_s > k_D$ always and $k_D < K_c$ when the crack stops propagating dynamically, every possible relative condition between the k's and the K's has been considered in the above discussion. We found that in so doing, the theory predicts all of the many facets of rupture in the earth, many of which had no prior explanation and further, that no phenomena have been observed that are not predicted. We thus now have a physical basis for understanding these phenomena. We can see why foreshock sequences may be variable, whereas

aftershock sequences are very regular. We have a physical explanation for the Omori Law, and we can see that since delayed multiple events are a special case and slow earthquakes, an even more special case, that these phenomena should be uncommon. The success of the theory in predicting the observations demonstrates that rupture in the earth obeys a law similar to that observed in the laboratory to result from stress corrosion. It does not, of course, prove that the causative mechanism is necessarily the same. What must be emphasized is that subcritical crack growth, governed by a rate equation of a type similar to eqn. (1) or (2), must play an important role in the earthquake mechanism, although the underlying mechanism(s) cannot with any surety be identified, and in principle may be unidentifiable.

MATHEMATICAL ANALYSIS

We develop here a very simple theoretical approach to calculate properties of stress-corrosion cracking. The stress-intensity factor k (defined by $\sigma = k/\sqrt{r}$, where σ = stress at the crack tip and r = distance from crack tip) for a two-dimensional plane crack (of any mode) and for a circular plane shear crack, in an infinite homogeneous medium which is linearly elastic everywhere off the crack plane, is given by

$$k = C \Delta\tau \sqrt{X} \tag{5}$$

where C is a geometric constant, $\Delta\tau$ is the static stress drop and X is the crack length for a two-dimensional crack and is the radius for a circular crack. C is equal to 1 for a two-dimensional shear or tensile crack [Lawn and Wilshaw, 1975]. For a circular shear crack, there are two modes (viz. Modes II and III) of propagation at a point along the crack edge, each with its own stress-intensity factor. Taking k to be the square-root of the sum of the squares of these two stress-intensity factors, C is given by $20/7\pi\sqrt{2}$ [Sih, 1973]. $\Delta\tau$ refers to a tensile or a shear stress component depending on the mode of crack propagation.

From experimental results on stress-corrosion cracking [Atkinson, 1979] we find

$$k = K_o\left(\frac{\dot{X}}{V_o}\right)^{1/n} \tag{6a}$$

or

$$k = W_o (\dot{X})^{1/n} \qquad (6b)$$

where K_o and V_o are the values of k and $\dot{X}$ at the initiation of quasistatic crack growth at time t = 0, and n is a dimensionless quantity called the 'stress-corrosion' index. K_o was discussed in detail in the introduction. The time t = 0 may actually refer to the time at which the crack velocity is no longer vanishingly small. W_o and n are the material properties of the medium. Combining (5) and (6a),

$$\dot{X} = V_o \left[\frac{C \, \Delta\tau \sqrt{X}}{K_o} \right]^n$$

If is independent of time, then $\dot{X} = V_o (\sqrt{\frac{X}{X_o}})^n \qquad (7)$

Integrating,

$$X = \left[X_o^{\frac{2-n}{2}} - \frac{n-2}{2} \frac{V_o t}{X_o^{n/2}} \right]^{\frac{2}{2-n}} \qquad (8)$$

The free parameters of this equation are X_o, V_o and n. The value of n (n is always > 2) at this point is simply taken from Atkinson [1979] but later we shall determine it. Note that Figure 1 shows that n is independent of temperature and humidity but (K_o, V_o) are not, so that in the earth we expect to find n to be close to Atkinson's result but (K_o, V_o) to be very different.

Using (8), we can find the time to failure (defined as the time from which the crack can be detected to start growing subcritically to when it reaches instability) simply by setting the quantity in square brackets equal to zero, since this is where $\dot{X}$ goes to infinity, since n >2. This is the 'nucleation time' of an earthquake. Time to failure is then given by

$$t_f = \frac{X_o}{V_o} \frac{2}{n-2} \qquad (9)$$

and the crack size X_f at time Δt before failure can be determined by substituting $t' = t_f - \Delta t$ into (8). The velocity at time Δt before failure can then be found from (7) by substituting X_f for X. Note that as long as $\Delta\tau$ is independent of time, it does not enter into equations (7), (8), and (9).

At this point let us point out an advantage of using (9) to determine time to failure t_f over the usual way of finding t_f [Evans, 1972]. t_f here depends only on the initial conditions and n and <u>not</u> on the final conditions. If we now assume a value for $\Delta\tau$, we can also calculate K_c just before failure. By following the above method, we have forced the crack to grow in accordance with a given $k - \dot{X}$ relationship (namely, equation (6)) until it reaches instability. The above method combines the two re-inforcing effects of the stress-corrosion instability with the geometric instability. Note that if the stress-corrosion index n and the point (K_c, V_c) of the (k-$\dot{X}$) curve at which the instability occurs are known, the subcritical rupture process cannot be determined, but if n and (K_o, V_o) are known, the total rupture process to instability can be completely determined. In this sense, K_o is a more fundamental property of the material than K_c for cases when stress-corrosion cracking occurs.

The formulation developed above is applicable to the case when the crack does reach instability. If the crack does not reach instability but propagates subcritically through a region of length L, say, then we need a minor modification of the method described above. As an example, let us consider the case of a pair of delayed multiple events, with the rupture length of the first rupture being X_o and with the barrier length between the two rupture zones being the length L. Then, combining equations (5) and (6b), we get the delay time between the multiple events to be

$$t_1 = \frac{2}{n-2} \left(\frac{W_o}{C\Delta\tau}\right)^n \left[X_o^{\frac{2-n}{2}} - (X_o + L)^{\frac{2-n}{2}} \right] \tag{10}$$

The unknown parameters in this equation are n, W_o, $\Delta\tau$, and L. If we have at least two sets of delayed multiple events across the same barrier (so that L, W_o, C, $\Delta\tau$, n are the same) but the rupture lengths of the first event of each set are different and the delay times for each pair are different, then we shall get a second equation like (10) with a different values of t_1, say t_2 and a different X_o, say X_o'. Dividing the two equations, we get

$$\frac{t_1}{t_2} = \frac{X_o^{\frac{2-n}{2}} - (X_o + L)^{\frac{2-n}{2}}}{X'^{\frac{2-n}{2}}_o - (X'_o + L)^{\frac{2-n}{2}}} \tag{11}$$

from which n can be obtained provided we assume a value for L. Once n is found, if we assume a $\Delta\tau$ and take K_o to be the stress-intensity factor due to a rupture of length X_o, we can also determine V_o from (10). In the above we used equation (1) together with (5) to derive the mathematical formulation of the problem. We also derived similar relations using (2) and (5) and our results of the later sections were found to be virtually the same, and so this case is not separately discussed.

We point out here that this method is valid only up to the point when the crack-edge velocity approaches the sonic wavespeeds of the medium. Once the crack propagates with velocities comparable to sonic, the problem becomes a dynamic problem and has to be treated as such.

In the next section, we shall use the method developed here to model in detail some of the scenarios described earlier.

THEORETICAL MODELLING OF NUCLEATION PHASE

In our calculations using the method of the previous section, we shall assume that the strength of the material along the zone through which the rupture actually proceeds to be constant, i.e., W_o and n are constants. Clearly, this will not be true in reality but since we do not know the details of this variation of strength, we do not think it meaningful at this time to complicate the model by introducing these variations. Our method, however, can be applied with minor modifications to the case of variable W_o and n. In that case the fault plane can be divided into segments of constant W_o and n (concentric ones for circular cracks) and our method can be applied individually to each section until instability is reached. It will generally be intuitively very clear what would happen if K_o were larger than the one chosen for the calculations.

We model the nucleation phase of the earthquake as a subcritical extension of a circular plane shear crack. The cases we consider are shown in Table 1. X_o, V_o and n are the input parameters. The values of V_o chosen were made consistent with the given n's, a stress drop $\Delta\tau$ of 100 bars, and a point (K_1, V_1) on the $(k\text{-}\dot{X})$ curve given by $K_1 = 10^{1.45}$ bar $\sqrt{\text{cm}}$; $V_1 = 0.1 \times 10^{-5}$ cm/sec for cases (i) and (ii), by $K_1 = 10^{1.85}$ bar $\sqrt{\text{cm}}$; $V_1 = 0.1 \times 10^{-5}$ cm/sec for cases (iii) and (iv); and by $K_1 = 10^{3.905}$ bar $\sqrt{\text{cm}}$, $V_1 = 0.1 \times 10^{-5}$ cm/sec for case (v). (However, we could also have chosen V_o arbitrarily.)

The values of K_1 [1 $MNm^{-3/2} = 10^2$ bar $\sqrt{\text{cm}}$] for cases (i) - (iv) are within the range shown in our Figure 1. The different cases represent different materials and the time to failure will tell us how strong they are. Using equations (8) and (9), the time to failure and the crack-radius X_f just before failure can be obtained. Let us take X_f to be the radius 1 second before failure. The results are shown in the last two columns of Table 1.

To study how the crack approaches instability in each case, we plot X vs. time from equation (8) for approximately the last 100 seconds before failure. The results are shown in Figures 4 and 6. The shape of the curves agree with those obtained in the laboratory by Wiederhorn [1967; Figure 2], and, more interestingly, with the dilatometer records of Sacks et al. [1981] reproduced in Figure 7. The curve of strain as a function of time just prior to an earthquake was found by these authors to be exactly of the form shown in Figures 4 and 6. For case (v), the velocity at the last few time steps is clearly comparable to sonic velocities of the medium so the values of t_f and X_f in this case are not exact. The crack radius increases very slowly until the last few time steps when it increases very rapidly. It is only during this last phase that any precursory strain change may be large enough to be detectable. However, other precursory phenomena may result indirectly from the quasistatic rupture growth during the nucleation phase.

In Figures 5 and 8 we plot the k-$\dot{X}$ curves along which the crack extends. We plot the point $(K_o,\dot{X}_o)$, $(K_1,\dot{X}_1)$ and the last three points at the last three seconds prior to failure on each curve. If K_c is the stress-intensity factor one second prior to failure, K_c is given by the topmost point on each $(k$-$\dot{X})$ curve. We have assumed $K_c \leq K_c^*$ in our calculations here. If $K_c > K_c^*$, the instability will occur earlier than we calculated, and X_f will be even smaller and the strain-change less detectable.

Thus our model of the nucleation phase of an earthquake implies that there must <u>always</u> be precursory slip and explains why it is seldom detected. We have assumed that only one crack is involved in the nucleation process. In reality there may be many small cracks growing subcritically and if enough cracks are involved in this process, the resulting strain change may be large enough to be measurable.

It is clear from Table 1 and Figures 4 and 6 that the size of the region over which the nucleation process occurs prior to the instability as well as the duration

of the nucleation process are highly dependent on the values of the variables assumed for the calculation. Therefore we have no idea at present as to either the spatial or temporal scale of the phenomenon, but can only make predictions as to its form. The scale can only be determined from observations such as those shown in Figure 7.

THEORETICAL MODELLING OF DELAYED MULTIPLE EVENTS

To search for this type of phenomenon we must look for two earthquakes with nearly adjacent rupture zones that occurred with a time delay t_D much longer than the rise time of an individual event but much shorter than the recurrence time, i.e., 10^1 sec << t_D << 10^{10} sec. Furthermore, the second event must be initiated in the region adjacent to the rupture zone of the first event, and propagate away from it. The second event of the pair is 'triggered' by the first and our theory suggests a physical mechanism by which one earthquake may 'trigger' another.

The Kii Peninsula barrier. Using an historical record that dates from 684 A.D., Ando [1975] has shown that this phenomenon has repeatedly occurred in large earthquakes along the Nankai trough in southwest Japan. He found that the plate boundary could be divided into four segments, A,B,C,D, that either rupture singly, in adjacent pairs, or all together in a single great earthquake (Figure 9). We show these regions in Figure 10 and note that Ando's observation indicates that the barriers between these regions are persistent, identifiable features. This is particularly true of the barrier of the tip of the Kii Peninsula, between regions C and B. Since 684 A.D., this barrier has been one end of the rupture zone of nine great earthquakes.

Ando also showed that the Kii Peninsula barrier has ruptured with a time delay four times during the historic record, producing four pairs of delayed multiple events. The most reliable record dates from 1707, when all four regions ruptured in a single event (Figure 9), thus resetting the initial conditions in all four regions at the same time. The next event was in 1854, when the Ansei I event

ruptured DC, followed 32 hours later by the rupture of BA in the Ansei II event. The next event was the Tonankai event of 1944, which ruptured C, followed two years later by the Nankaido earthquake, which ruptured B dynamically and A quasistatically. Ando was able to show clearly that the Nankaido earthquake initiated near the BC boundary and propagated to the west, as predicted.

These two sets of delayed multiple events (1854 and 1944-46) ruptured the same barrier quasistatically and this provides us with a unique opportunity for calculating n for this barrier. The required model parameters for quantitative modelling of these earthquake pairs are taken from Ando, and shown below using our previous notation.

Ansei I-II pair	Tonankai - Nankaido pair
t_1 = 32 hours	t_2 = 750 days
X_o = 230 km	X'_o = 133 km

Let us solve the problem using the various values of L shown in Table 2. For each case, the calculated n is shown in the second column.

We see that the value of n is virtually independent of L. More importantly, n differs from the value found by Atkinson only by a factor of 1 or 2. This is a remarkable agreement considering the simplicity of our model and the fact that we model a Mode II crack while Atkinson's crack propagated mainly in Mode I. If we assume $\Delta\tau$ = 100 bars, and take K_o to be the stress-intensity factor due to a rupture of length 230 km, we can determine V_o from (10).

For the multiple event to occur, the barrier must have a strength such that $K_o \leq k_s$. For the cases studied here, X_o = 100 km and $\Delta\tau$ = 100 bars, so that $K_o \leq 10^3$ bar $km^{1/2}$. The specific fracture energy is given by $G = K^2/4\mu$ [Lawn and Wilshaw, 1975], so that $G \cdot 10^{11}$ erg/cm^2. This value, similar to that obtained by

Aki [1979] for the Fort Tejon earthquake, is very high, implying kilobars of shear stress in the vicinity of the crack tip, and a specific surface energy much higher than that of any known material, therefore care should be taken in interpreting its meaning. It seems reasonable to suggest that this energy is dissipated in inelastic deformation within some volume surrounding the crack tip. This is a natural extension of the 'end zone' concept of Barenblatt [1959] discussed by Aki [1979] in his treatment of the subject. A pronounced change in the dip of the Benioff zone associated with the Nankai trough occurs beneath the Kii Peninsula, hence it is likely that this barrier is caused by a jog in the rupture plane (K. Mogi, personal communication, 1980). We envision that the energy required to stop the rupture is dissipated in the volume behind the jog.

Our estimate of K_o for the Kii Peninsula barrier is several orders of magnitude higher than that assumed in our discussion of the nucleation problem. We would therefore not expect nucleation to occur within such an anomalous region, as excessive time (or stress) would be required. Variation in K_o or K_c by orders of magnitude was also found by Aki [1979]. This suggests to us that these variations are due to geometrical complexities of the fault zone, rather than changes in the properties of the fault zone materials which are unlikely to vary so widely. It is interesting that, as discussed earlier with respect to heterogeneity, such geometric irregularly is expected to increase as $X^{1/2}$, which is exactly the manner in which k scales (at constant $\Delta\sigma$). This suggests that the probability for an earthquake to stop will be scale independent.

An Example and Counterexample from the Aleutians

We now turn to several other examples of delayed multiple events that illustrate other aspects of the phenomenon. In Figure 11 we show the space time

sequence of large earthquakes in the Aleutian arc [from Sykes et al., 1980]. We see one clear example of a delayed multiple event: the 1957 Central Aleutians earthquake was followed 7 years later by the Rat Island earthquake, which initiated at the end of the 1957 rupture zone and propagated to the west [Sykes, 1971]. The barrier in this case, and in the case of most regions in the Aleutians where the rupture zones of large earthquakes terminate, has strong expression in the bathymetry [Spence, 1977].

It might, on first inspection, also appear from Figure 11 that the November 10, 1938 earthquake and the 1964 Alaskan earthquake are another example of a delayed multiple event pair. This is not the case, however, because the 1964 event initiated in the northeast part of its rupture zone and propagated to the southwest, i.e., towards the rupture zone of the earlier event. Therefore the close occurrence in time of these two contiguous events is a coincidence.

A Second Type of Aftershock Sequence

We note one additional interesting example from the Aleutians. The Rat Island earthquake of 1965 was followed by a sequence of large normal faulting earthquakes in the adjacent outer wall of the trench [Stauder, 1968]. This type of earthquake results from flexure of the outer wall and rise resulting from subduction [Sykes, 1971]. The sudden subduction produced by the Rat Island earthquake would be expected to 'trigger' earthquakes in the outer wall because it would result in a sudden increase in the flexure and it would also result in a sudden reduction in the horizontal compressive stress in the outer rise. Thus k would be increased for normal faults in the outer rise as a result of the Rat Island earthquake, and for any region in which $K_o < k < K_c$, failure will occur after a time delay. These events are therefore aftershocks of the Rat Island earthquake,

but of a different type than discussed earlier. The largest event in this sequence was an event of $M_s = 7.5$ which occurred 57 days after the Rat Island earthquake. This is thus a minimum estimate of the nucleation time for this earthquake. (It is a minimum estimate because our earlier definition of nucleation time was that it is the time to the instability from the initial condition $k = K_o$.)

Complex Events

In the above example, the difference between aftershocks and delayed multiple events is less distinct than in the usual case. The delayed multiple events discussed above are cases in which the two events occurred on the same fault. Cases of multiple events in which the two events occurred on different faults have also been observed. Delayed multiple events occur commonly in the Solomon Islands, and some of these occur near the sharp corner of the trench near New Britain and go around the corner [Lay and Kanamori, 1980; McCann, 1980]. Thus the first event has a N-S strike, the second E-W, or vice versa. Lay and Kanamori [1980] argue that this indicates that the slab is continuous around the corner, but this need not be so. The two Gazli earthquakes of 1976 occurred on two conjugate thrust faults with a time delay of 39 days, and certainly in this case an argument that they occurred on the same fault would be a forced one [Kristy et al., 1980]. There does not need to be a delay in such complex events, however. The 1927 Tango earthquake ruptured two orthogonal, conjugate, strike-slip faults in SW Japan. It is not known, however, whether this was a normal multiple event in which both faults ruptured dynamically or if one fault ruptured dynamically, the other quasistatically. We certainly know that it is possible for the first event to rupture dynamically and the second quasistatically on different faults, since this phenomenon was observed to follow the 1968 Borrego Mountain earthquake in

California [Allen et al., 1972]. The earthquake, which was on the San Jacinto fault, triggered quasistatic slip on the nearby Superstition Hills, Imperial, and San Andreas faults. Although we are not presently prepared to model these complex cases quantitatively, we believe they result from the same physical mechanism as discussed above.

The Effect of the Phase of the Loading Cycle

The loading cycle for a given region is the time required for the tectonic process to replenish the stress dropped in the previous earthquake on the same section of fault plane. The period of this cycle is the recurrence time for earthquakes in that place. It is clear from the above that the condition for the occurrence of multiple events and delayed multiple events is that the two regions on either side of the barrier must be nearly in phase in their loading cycles. We might expect, then, to see adjoining regions going in and out of phase in a cycle much longer than the loading cycle. Indeed, two such phase cycles appear in Ando's history (Figure 10). We begin in 887 A.D., when an ABCD event occurred, setting all regions into phase. This was followed by two delayed multiple events: the 1096 A.D. - 1099 A.D. pair and the 1360 A.D. -1361 A.D. pair. Then the 1498 A.D. CD event occurred, with no corresponding BA event, suggesting that BA was too far out of phase to be ruptured as a delayed event. The BA region ruptured 107 years later in 1605 A.D. The ABCD event of 1707 again put the regions in phase. Next follows the Ansei I and II pair, and the Tonankai-Nankaido pair. The regions seem to be getting out of phase again because D did not rupture in the most recent sequence. This region (Suruga Bay and the Tokai district) will either rupture on its own, which has not been observed to happen before, or skip this cycle and rupture in the next ABCD or CD event.

The reason we expect such phase cycles to occur is that two competing effects are at work. The first is the rupture process itself, which simply by it producing rupture on all possible regions in a given event, has a smoothing effect on heterogeneity which results in high phase correlation of adjoining regions. On the other hand, spatial variation of the tectonic process, such as variation in the slip vector magnitude and direction along a plate boundary, and heterogeneity of the geometry and material properties of the fault zone have a roughening effect. The first effect produces strong clustering in a space-time sense, the second randomness. What results, and is observed, is weak clustering. This is why space-time diagrams, such as those of Kelleher et al. [1970] seldom show significant or clearly obvious trends.

CONCLUSIONS

We have presented a detailed discussion of subcritical crack growth and its application to time-dependent rupture in the earth. Using very basic concepts of fracture mechanics and results obtained from laboratory experiments, we found that our theory predicts various scenarios for time-dependent rupture in the earth. We have presented several examples to show that all of the predicted phenomena are actually observed in the earth. The theory does not contain any predictions other than those observed to occur, nor do the observations indicate that any phenomena occur other than those predicted. Our theory explains why some of these phenomena are more common than others. Using a simple theoretical development, we model two cases in detail, the nucleation stage before an earthquake and delayed multiple events. For the nucleation problem we show that all earthquakes must have precursory slip but the resulting strain changes may be much too small to be detectable. For delayed multiple events occurring along the Nankai trough, we found two pairs of delayed mutliple events that were separated by the same barrier. We uniquely determined an estimate of the stress corrosion index for the barrier between these events. We thus obtained estimates of the material properties of barriers in the earth. Our theory also suggests a physical mechanism by which an earthquake can 'trigger' another earthquake on an adajcent zone of the same fault or on a different fault in its vicinity.

Acknowledgments. We would like to thank Paul Richards and Lynn Sykes for critically reviewing the manuscript. Selwyn Sacks allowed us to reproduce Figure 7 prior to its publication and we are grateful to him for this. This work was supported by National Aeronautics and Space Administration grant NGR 33-008-146, and National Science Foundation, Division of Earth Sciences, grants EAR-79-01810 and EAR-80-07426. Lamont-Doherty Geological Observatory Contribution No. 0000.

REFERENCES

Achenbach, J. D., On dynamic effects in brittle fracture, Mechanics Today, Pergamon Press, New York, 1973.

Aki, K., Characteristics of barriers on an earthquake fault, J. Geophys. Res., 84, 6140-6148, 1979.

Allen, C. R., M. Wyss, J. Brune, A. Grantz, and R. Wallace, Displacement on the Imperial, Superstition Hills, and San Andreas faults triggered by the Borrego Mtn. earthquakes, in The Borrego Mtn. Earthquake of April 9, 1968, U. S. Geol. Surv. Prof. Paper 787, 55-87, 1972.

Ando, M., Source mechanisms and tectonic significance of historical earthquakes along the Nankai trough, Japan, Tectonophysics, 27, 119-140, 1975.

Andrews, D. J., Rupture velocity of plane strain shear cracks, J. Geophys. Res., 81, 5679-5687, 1976.

Atkinson, B. K., A fracture mechanics study of subcritical tensile cracking of quartz in wet environments, Pure Appl. Geophys., 117, 1011-1024, 1979.

Barenblatt, G. I., The formation of equilibrium cracks during brittle fracture: General ideas and hypotheses, axially symmetric cracks, J. Appl. Math. Mech., 23, 434-444, 1959.

Das, S., and K. Aki, A numerical study of two-dimensional rupture propagation, Geophys. J. R. astr. Soc., 50, 643-668, 1977a.

Das, S., and K. Aki, Fault plane with barriers: A versatile earthquake model, J. Geophys. Res., 82, 5658-5670, 1977b.

Davies, J., L. Sykes, L. House, and K. Jacob, Shumagin Seismic Gap, Alaska Peninsula: History of great earthquakes, tectonic setting, and evidence for high seismic potential, to be submitted to J. Geophys. Res., 1980.

Dieterich, J. H., Time-dependent friction and the mechanics of stick-slip, Pure Appl. Geophys., 116, 790-806, 1978.

Evans, A. G., A method for evaluating the time-dependent failure characteristics of brittle materials - and its application to polycrystalline alumina, J. Mat. Sci., 7, 1137-1146, 1972.

Fossum, A. F., and L. B. Freund, Nonuniformly moving shear crack model of a shallow focus earthquake and mechanism, J. Geophys. Res., 80, 3343-3347, 1975.

Freund, L. B., The mechanics of dynamic shear crack propagation, J. Geophys. Res., 84, 2199-2209, 1979.

Kanamori, H., Mechanism of tsunami earthquakes, Phys. Earth Planet. Int., 6, 346-359, 1972.

Kanamori, H., and J. J. Cipar, Focal process of the great Chilean earthquake May 22, 1960, Phys. Earth. Planet. Int., 9, 128-136, 1974.

Kanamori, H., and G. S. Stewart, A slow earthquake, Phys. Earth. Planet. Int., 18, 167-175, 1979.

Kelleher, J. A., Space-time seismicity of the Alaska-Aleutian Seismic Zone, J. Geophys. Res., 75, 5745-5756, 1970.

Knott, J. F., Fundamentals of Fracture Mechanics, John Wiley, 1973, 273 pp.

Kostrov, B. V., Unsteady propagation of longitudinal shear cracks, J. Appl. Math. Mech., 30, 1241-1248, 1966.

Kostrov, B. V., Nikitin, and L. M. Flitman, The mechanics of brittle fracture, Mech. Solids, 3, 105-117, 1969.

Kostrov, B. V., Seismic moment and energy of earthquakes, and seismic flow of rock, Izv., Earth Physics, No. 1, 23-40, 1974.

Kranz, R. L., The effects of confining pressure and stress differences on static fatigue of granite, J. Geophys. Res., in press, 1980.

Kranz, R. L., and C. H. Scholz, Critical dilatant volume of rocks at the onset of tertiary creep, J. Geophys. Res., 82, 4893-4898, 1977.

Kristy, M. J., L. J. Burdick, and D. W. Simpson, The focal mechanisms of the Gazli, USSR earthquakes, Bull. Seismol. Soc. Amer., in press, 1980.

Lawn, B. R., and J. R. Wilshaw, Fracture of Brittle Solids, Cambridge Univ. Press, 1975.

Lay, T., and H. Kanamori, Earthquake doublets in the Solomon Islands, Phys. Earth Planet. Int., 21, 238-304, 1980.

Mandelbrot, B., Fractals, W. H. Freeman, San Francisco, 1977.

Martin, R. J., III, Time-dependent crack growth in quartz and its application to the creep of rocks, J. Geophys. Res., 77, 1406-1419, 1972.

McCann, W. R., Seismic potential and seismic regimes of the southwest Pacific, submitted to J. Geophys. Res., 1980.

Mould, R. E., and R. D. Southwick, Strength and static fatigue of abraded glass under controlled ambient conditions, J. Amer. Ceram. Soc., 42, 582, 1959.

Page, R., Aftershocks and microearthquakes of the Great Alaska earthquake of 1964, Bull. Seism. Soc. Am., 58 (3), 1131-1168, 1968.

Reid, H. F., The mechanics of the earthquake, the California earthquake of April 18, 1906, Report of the State Investigation Commission, 2, Carnegie Inst. Washington, Washington, D.C., 1910.

Richards, P. G., Dynamic motions near an earthquake fault: A three-dimensional solution, Bull. Seismol. Soc. Amer., 65, 93-112, 1976.

Sacks, I. S., Borehole strainmeters, Proc. USGS Conf. VII: Stress and Strain Measurements Related to Earthquake Prediction, Sept. 7-9, 1978 San Francisco, 425-448, 1978.

Sacks, I. S., A. T. Linde, S. Suyehiro, and J. A. Snoke, Anelastic redistribution of stress, 3rd M. Ewing Symp., New Paltz, New York, May 1980.

Sacks, I. S., S. Suyehiro, A. T. Linde, and J. A. Snoke, Slow earthquakes and stress redistribution, Nature, 275, 599-602, 1978.

Sacks, I. S., S. Suyehiro, A. T. Linde, and J. A. Snoke, Stress redistribution and slow earthquakes, submitted to Tectonophysics, 1981.

Sayles, R., and T. Thomas, Surface topography as a nonstationary random process, Nature, 271, 431-434, 1978.

Scholz, C. H., Mechanism of creep in brittle rock, J. Geophys. Res., 73, 3295-3302, 1968a.

Scholz, C. H., Microfractures, aftershocks, and seismicity, Bull. Seismol. Soc. Amer., 58, 1117-1130, 1968b.

Scholz, C. H., Static fatigue of quartz, J. Geophys. Res., 77, 2104-2114, 1972a.

Scholz, C. H., Crustal movements in tectonic areas, Tectonophysics, 14, 201-217, 1972b.

Scholz, C. H., and J. T. Engelder, The role of asperity indentation and ploughing in rock friction, I. Asperity creep and stick-slip, Int. J. Rock Mech. Mining Sci., 13, 149-154, 1976.

Sih, G. C., Handbook of Stress-Intensity Factors, Inst. Fracture and Solid Mechanics, LeHigh Univ., Bethlehem, Pa., 1973.

Smith, S. W., and M. Wyss, Displacement on the San Andreas fault initiated by the 1966 Parkfield earthquake, Bull. Seismol. Soc. Amer., 58, 1955-1974, 1968.

Spence, W., The Aleutian Arc: Tectonic blocks, episodic subduction, strain diffusion, and magma generation, J. Geophys. Res., 82, 213-230, 1977.

Stauder, W., Mechanism of the Rat Island earthquake sequence of February 4, 1965, with relation to island arcs and sea-floor spreading, J. Geophys. Res., 73, 3847- , 1968.

Sykes, L. R., Aftershock zones of great earthquakes, seismicity gaps, and earthquake prediction for Alaska and Aleutians, J. Geophys. Res., 76, 8021-8041, 1971.

Sykes, L., J. Kisslinger, L. House, J. Davies, and K. H. Jacob, Rupture zones of great earthquakes, Alaska-Aleutian Arc, 1784-1980, submitted to Science, 1980.

Utsu, T., Aftershocks and earthquake statistics, I: J. Fac. Sci., Hokkaido Univ., 3, 129-194, 1969.

Utsu, T., Aftershocks and earthquake statistics, II:, J. Fac. Sci., Hokkaido Univ., 3, 197-266, 1970.

Utsu, T., Aftershocks and earthquake statistics, III:, J. Fac. Sci., Hokkaido Univ., 3, 399-441, 1971.

Utsu, T., Aftershocks and earthquake statistics, IV:, J. Fac. Sci., Hokkaido Univ., 3, 1-42, 1972.

Wiederhorn, S. M., Influence of water vapor on crack propagation in soda-lime glass, J. Amer. Ceram. Soc., 50, 407-414, 1967.

Wiederhorn, S. M., and L. H. Bolz, Stress corrosion and static fatigue of glass, J. Amer. Ceram. Soc., 53, 543, 1970.

Wyss, M., and J. N. Brune, The Alaska earthquake of 28 March, 1964: A complex multiple rupture, Bull. Seismol. Soc. Amer., 57, 1017-1023, 1967.

TABLE 1

Stress-Corrosion Index, n	Initial Crack Radius, X_o	Initial Crack-Edge Velocity, V_o, cm/sec	Time to Failure, t_f	Crack Radius 1 Second Before Failure, X_f
12.5	0.1 cm	0.169×10^{-7}	1125906 sec ≈ 13.0 days	1.76 cm
20.0	0.1 cm	0.146×10^{-8}	7593035 sec ≈ 87.9 days	0.63 cm
12.5	0.5 cm	0.395×10^{-8}	24094025 sec ≈ 278.9 days	14.18 cm
20.0	0.5 cm	0.143×10^{-9}	388763365 sec ≈ 12.3 yr	5.69 cm
12.5	1.0 km	0.1099	173382 sec ≈ 2.0 days	1.4 km

TABLE 2

Barrier-width L (km)	Stress-corrosion Index (n)
1.	23.2
10.	23.8
20.	24.2
50.	24.8

FIGURE CAPTIONS

Figure 1. Experimental data obtained by Atkinson [1979] for single crystal quartz showing relationship between stress-intensity factor k and crack tip velocity for subcritical rupture for Mode I cracks.

Figure 2. Schematic diagram showing the nucleation phase of an earthquake and the resulting phenomena. X denotes the distance along the crack, u the corresponding slip, and β an elastic wave velocity. Stipling denotes subcritical rupture and hatching denotes dynamic rupture. The sawtooth in case A indicates the presence of a barrier, i.e., a region in which rupture is relatively inhibited. The conditions on k in the two cases are indicated. A slow earthquake arises when the rupture propagates into regions in which $k < K_o$. In the more likely case, an instability arises and a 'normal' earthquake occurs.

Figure 3. Schematic diagram using the same symbolism as Figure 2 showing how earthquakes stop and the resulting phenomena. The earthquake stops at a barrier when $k_D < K_c$ for the barrier. As the slip between the barriers tends to its static value, k increases to k_s. If the barrier has uniform strength, then either $k_s < K_o$, $K_o < k_s < K_c$ or $k_s > K_c$ and we have cases A, B, or C. If the barrier increases in strength with distance, case D occurs. Case E shows the aftershock that occurs as a result of non-uniform slip on the fault.

Figure 4. Diagrams showing the crack-radius as a function of time during the nucleation phase. The star denotes initial crack size.

Figure 5. Stress intensity factor k as a function of crack edge velocity $\dot{X}$ for the cases shown in Figure 4. The last three points on each curve denote the values of k and $\dot{X}$ three seconds prior to failure. The last point is a very good estimate of K_c, the modulus of cohesion for stress corrosion cracking.

Figure 6. Same as Figure 4, but showing case (v)..

Figure 7. Plot of strain vs. time recorded with a dilatometer due to a nearby small earthquake in the Matsushiro region. The event 74/07/24 is preceded by a slow strain change which accelerates into a 'normal' earthquake. The earthquake onset is shown by the arrow. Compare the form of the precursor with Figures 4 and 6 [after Sacks et al., 1981].

Figure 8. Same as Figure 5, but showing one case (v). $\dot{X}$ is in km/hr. In this case, the $\dot{X}$ at the last few points is comparable to the sonic velocity of the medium, so that the quasistatic rupture theory is no longer valid and the estimate of K_c is not very reliable.

Figure 9. Schematic representation of earthquakes along the Nankai trough, western Japan, since 684 A.D. (modified from Ando [1975]). Since 1707 A.D., further details are included. The rupture lengths of the first event of an event pair and the delay times between pairs are

shown. The arrows indicate that the second rupture initiated from the end where the first rupture had been arrested by the barrier.

Figure 10. Bathymetric map off the southeast coast of Japan showing the segments A,B,C,D along the Nankai trough. The barriers between the segments may have some weak correlation with the bathymetry.

Figure 11. Map of rupture zones and the space time sequence of large earthquakes along the Aleutian arc [after Davies et al., 1980 and Sykes et al., 1980]. We make specific reference to the adjacent 1957 and 1965 events, which are delayed multiple events, and the 1938 and 1964 pair, which are not.

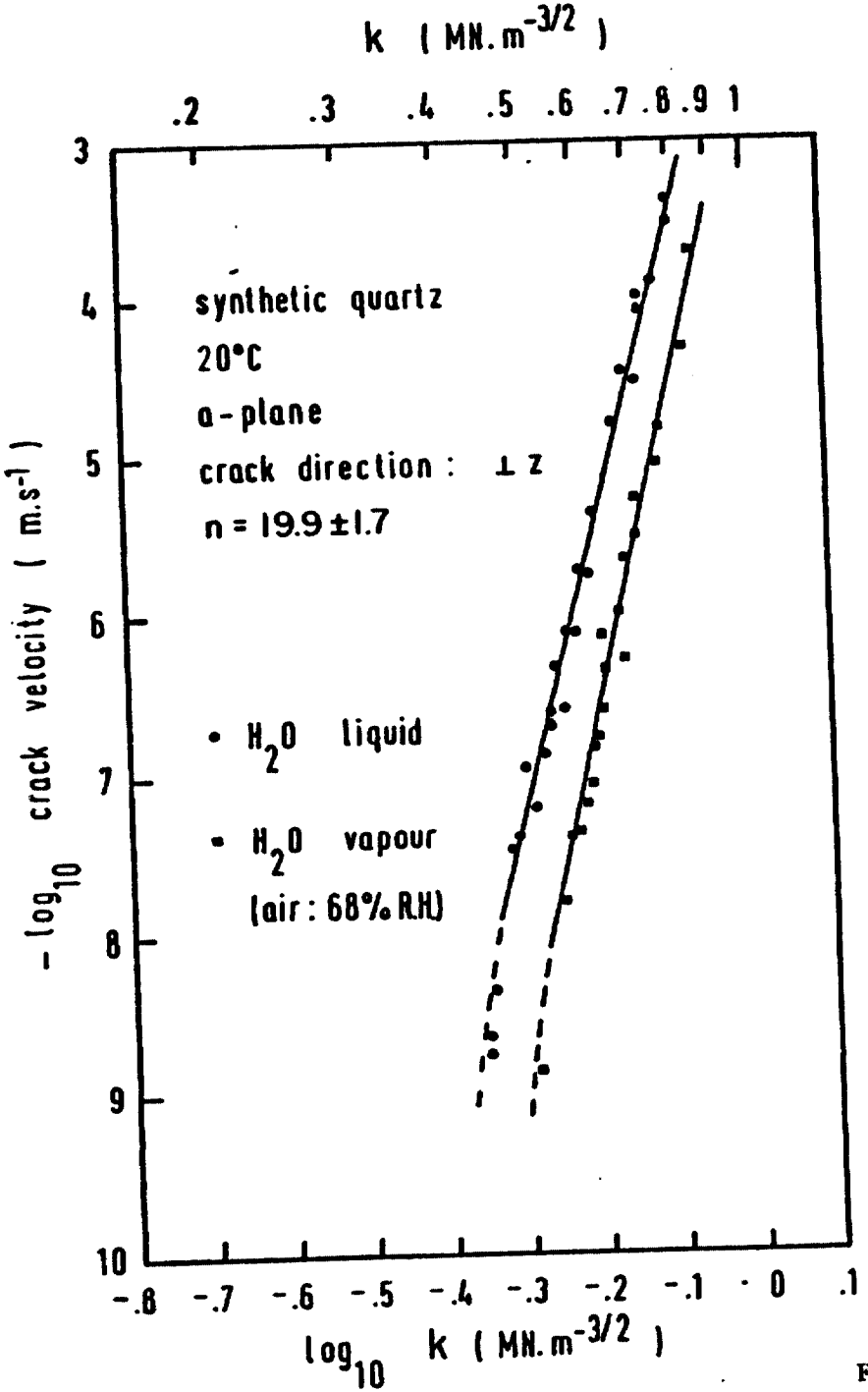
k (MN.m$^{-3/2}$)
.2 .3 .4 .5 .6 .7 .8 .9 1
synthetic quartz
20°C
a-plane
crack direction : ⊥ z
n = 19.9 ± 1.7
• H_2O liquid
• H_2O vapour
(air : 68% R.H)
$-\log_{10}$ crack velocity (m.s^{-1})
3 4 5 6 7 8 9 10
-.8 -.7 -.6 -.5 -.4 -.3 -.2 -.1 0 .1
$\log_{10}$ k (MN.m$^{-3/2}$)

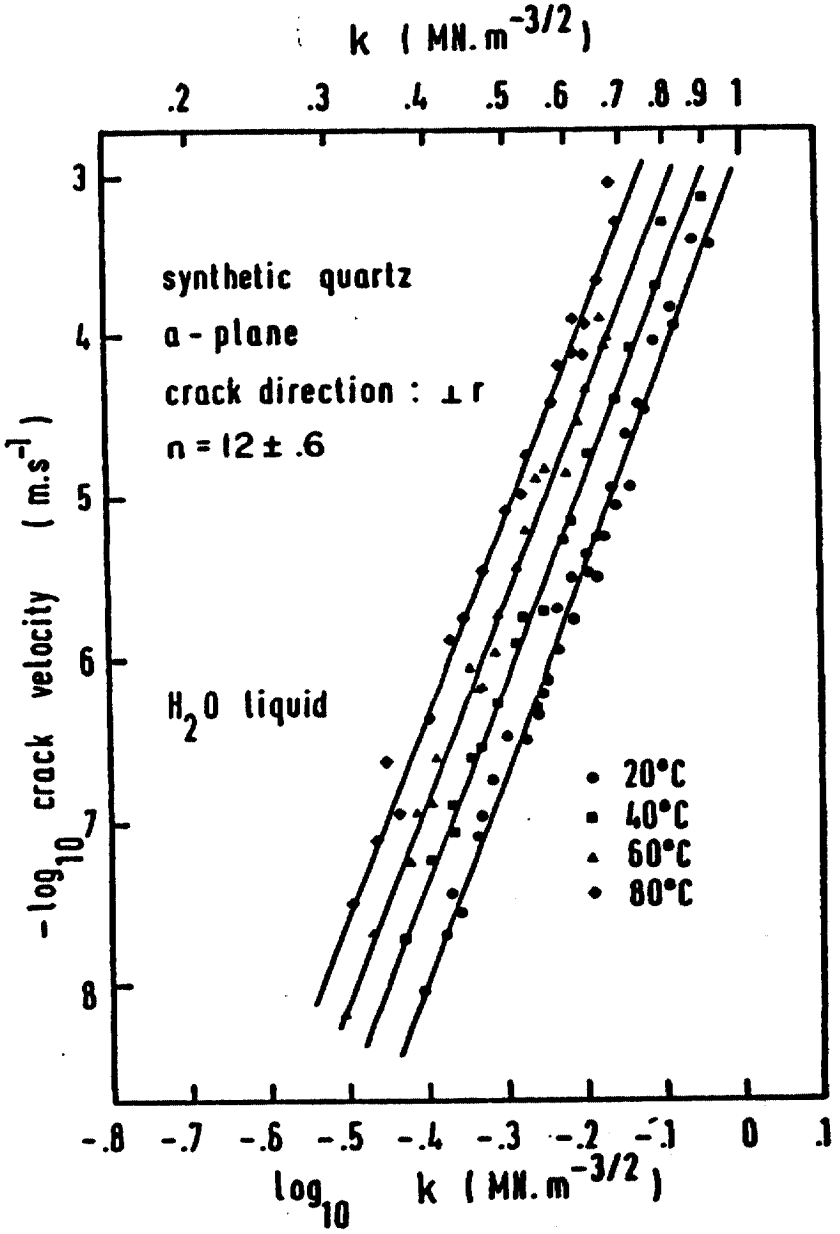
k (MN.m$^{-3/2}$)
.2 .3 .4 .5 .6 .7 .8 .9 1
synthetic quartz
a-plane
crack direction : ⊥ r
n = 12 ± .6
H_2O liquid
• 20°C
▪ 40°C
▲ 60°C
◆ 80°C
$-\log_{10}$ crack velocity (m.s^{-1})
3 4 5 6 7 8
-.8 -.7 -.6 -.5 -.4 -.3 -.2 -.1 0 .1
$\log_{10}$ k (MN.m$^{-3/2}$)

Figure 1

I Nucleation

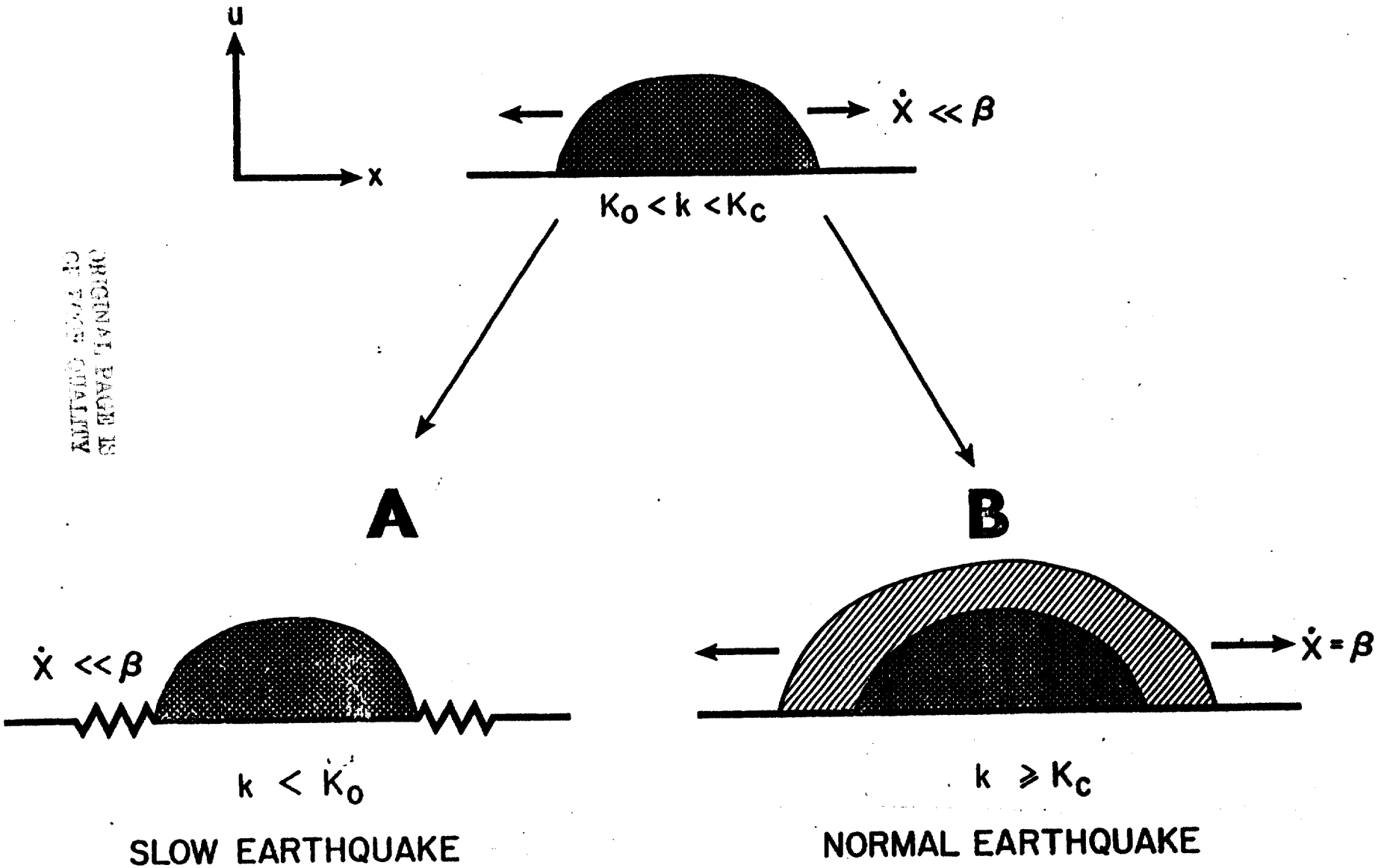

Figure 2

II Stopping

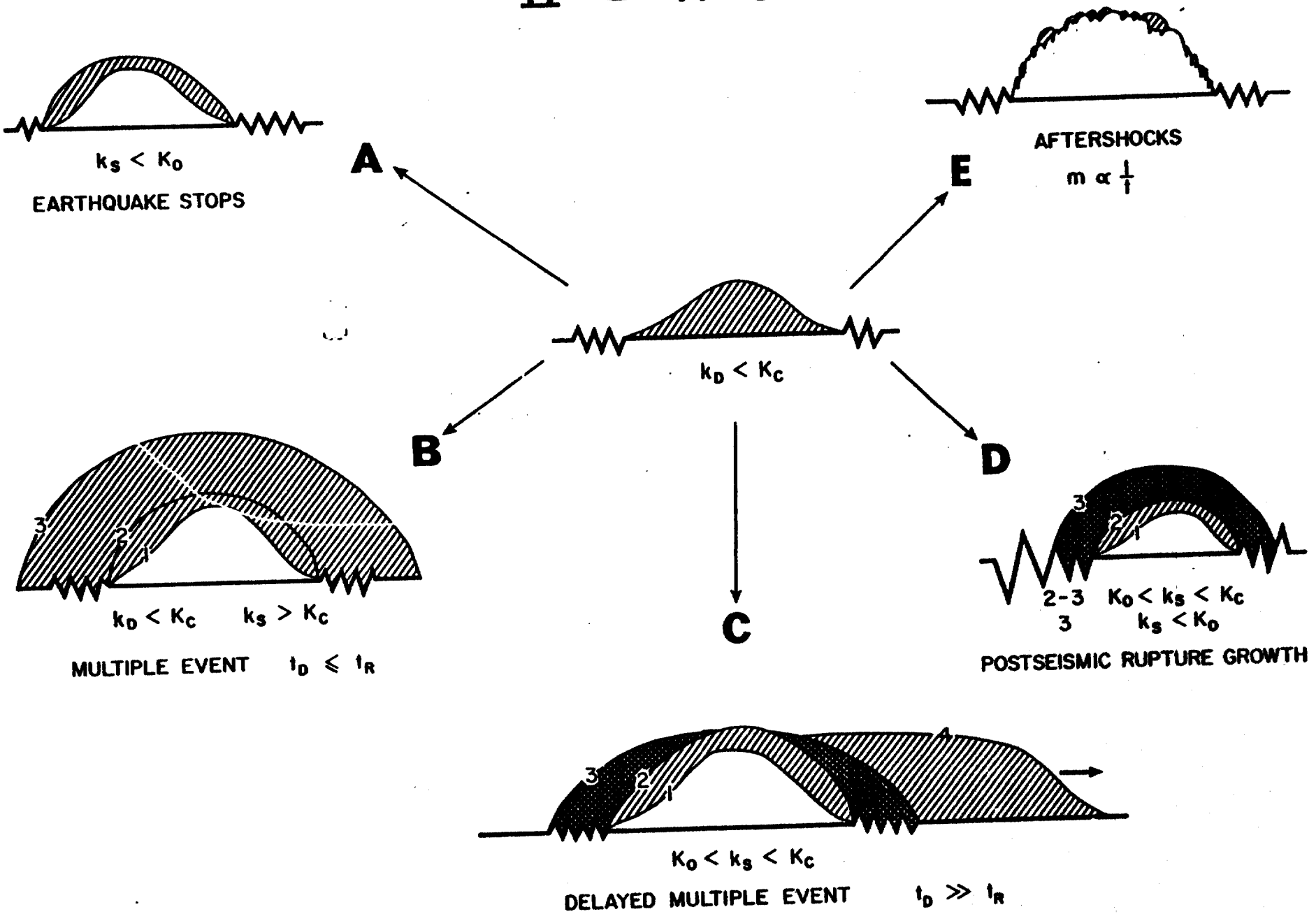

Figure 3

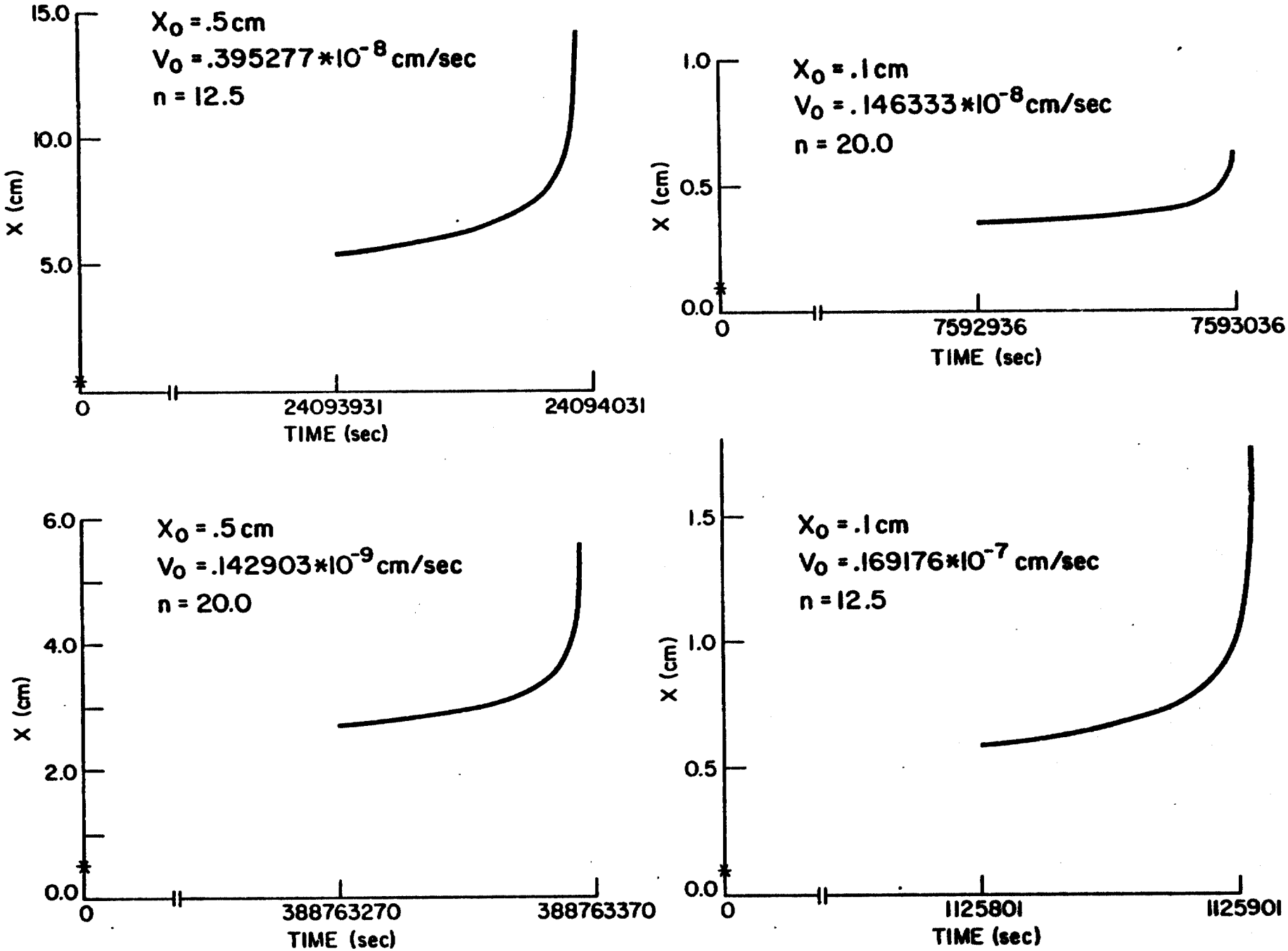
15.0
10.0
5.0
X (cm)
X_0 = .5 cm
V_0 = .395277 * 10^{-8} cm/sec
n = 12.5
0
24093931
24094031
TIME (sec)
1.0
0.5
0.0
X (cm)
X_0 = .1 cm
V_0 = .146333 * 10^{-8} cm/sec
n = 20.0
0
7592936
7593036
TIME (sec)
6.0
4.0
2.0
0.0
X (cm)
X_0 = .5 cm
V_0 = .142903 * 10^{-9} cm/sec
n = 20.0
0
388763270
388763370
TIME (sec)
1.5
1.0
0.5
0.0
X (cm)
X_0 = .1 cm
V_0 = .169176 * 10^{-7} cm/sec
n = 12.5
0
1125801
1125901
TIME (sec)

Figure 4

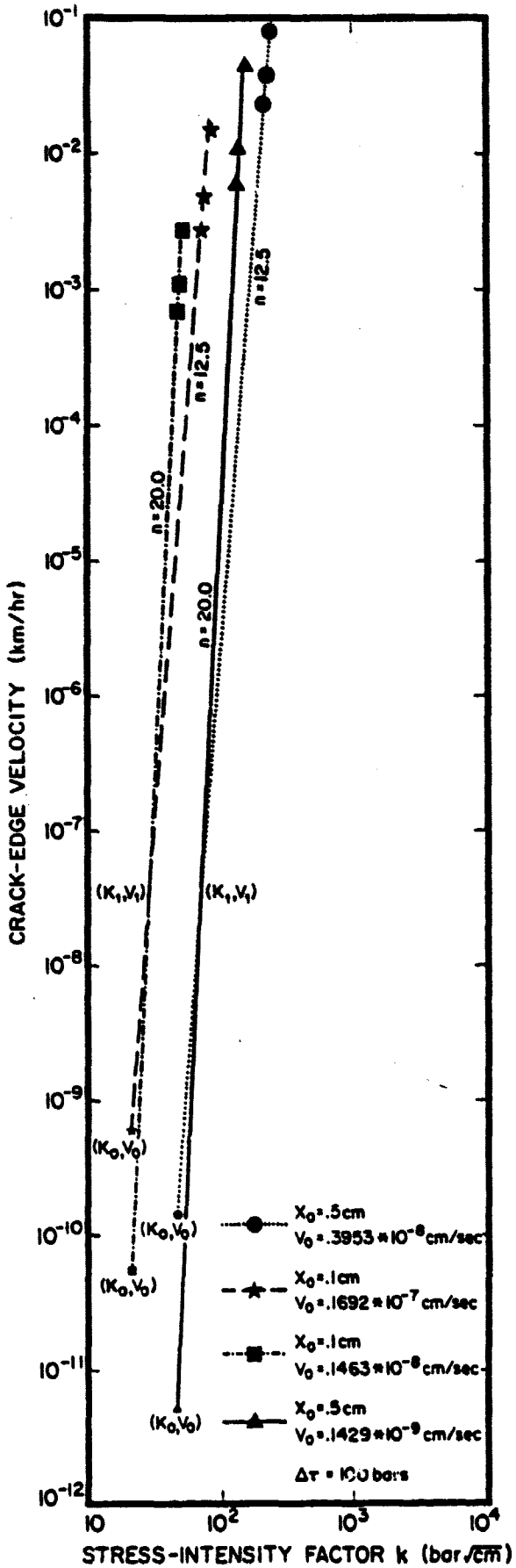
CRACK-EDGE VELOCITY (km/hr)
STRESS-INTENSITY FACTOR k (bar√cm)
n=20.0
n=12.5
n=12.5
n=20.0
(K1,V1)
(K1,V1)
(K0,V0)
(K0,V0)
(K0,V0)
(K0,V0)
X0=.5cm
V0=.3953*10-8cm/sec
X0=.1cm
V0=.1692*10-7cm/sec
X0=.1cm
V0=.1463*10-8cm/sec
X0=.5cm
V0=.1429*10-9cm/sec
Δτ = 100 bars

Figure 5

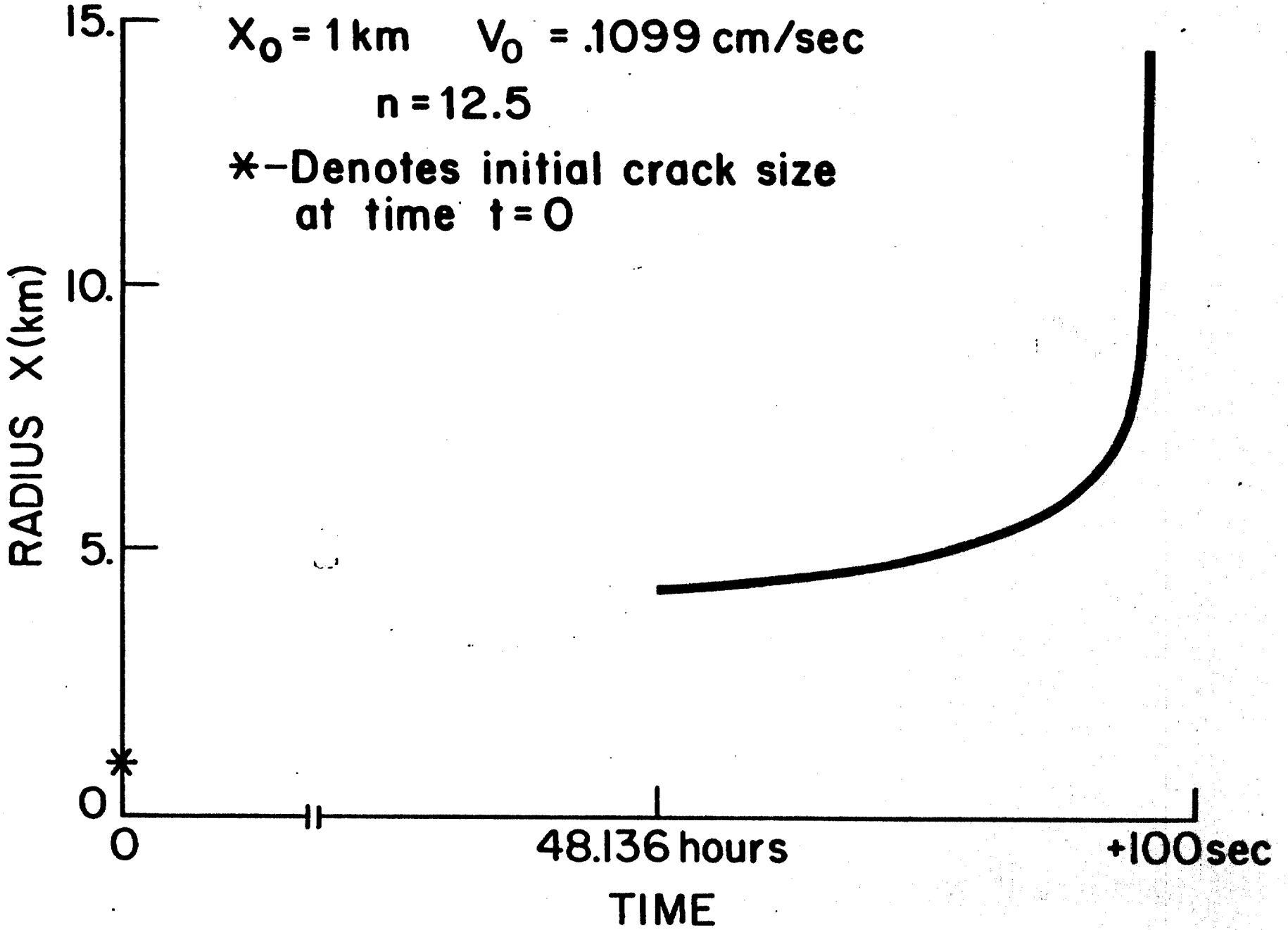
15.
10.
5.
0
RADIUS X(km)
X_0 = 1 km V_0 = .1099 cm/sec
n = 12.5
*–Denotes initial crack size at time t = 0
0
48.136 hours
+100 sec
TIME

Figure 6

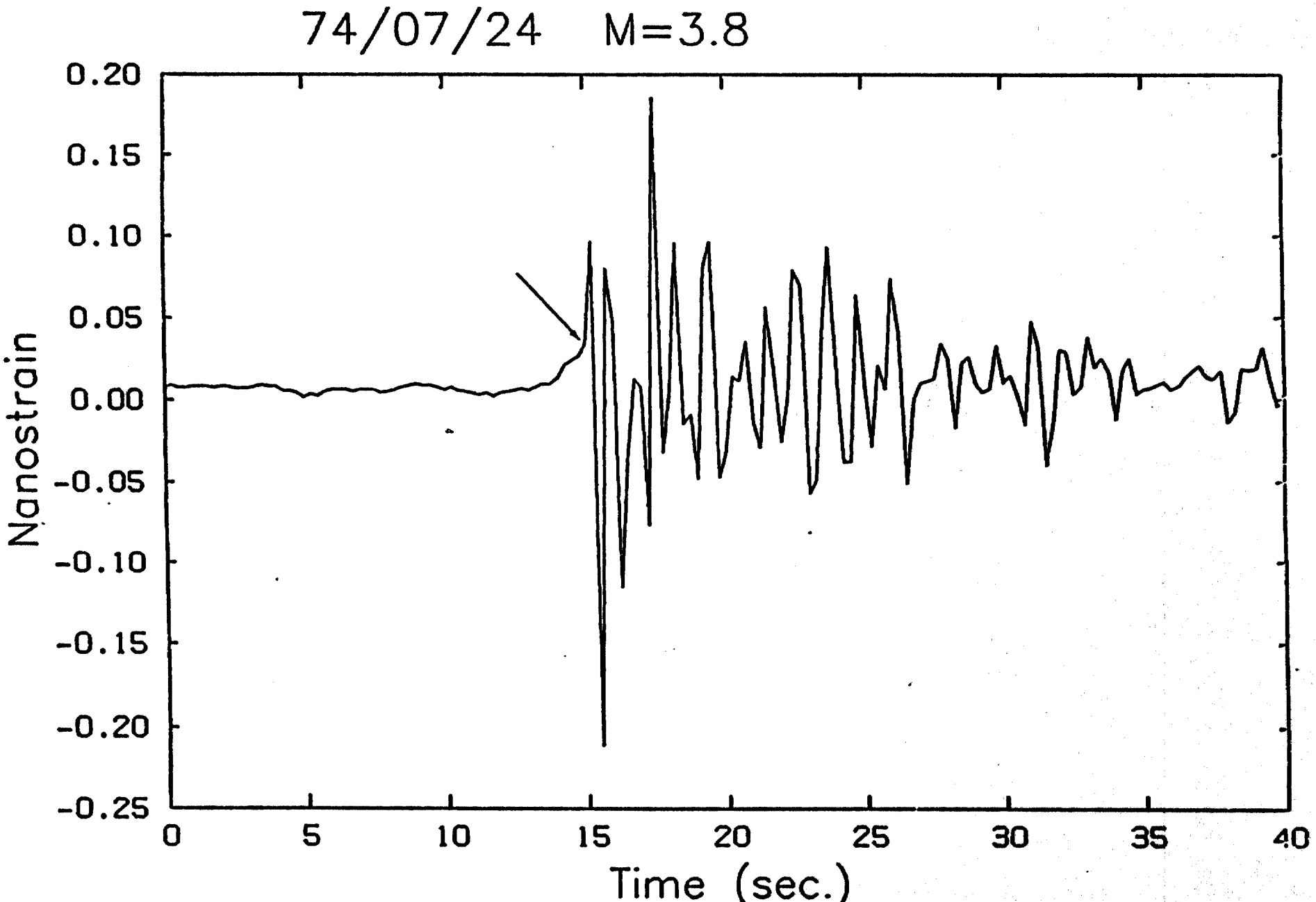
74/07/24 M=3.8
0.20
0.15
0.10
0.05
0.00
-0.05
-0.10
-0.15
-0.20
-0.25
Nanostrain
0
5
10
15
20
25
30
35
40
Time (sec.)

Figure 7

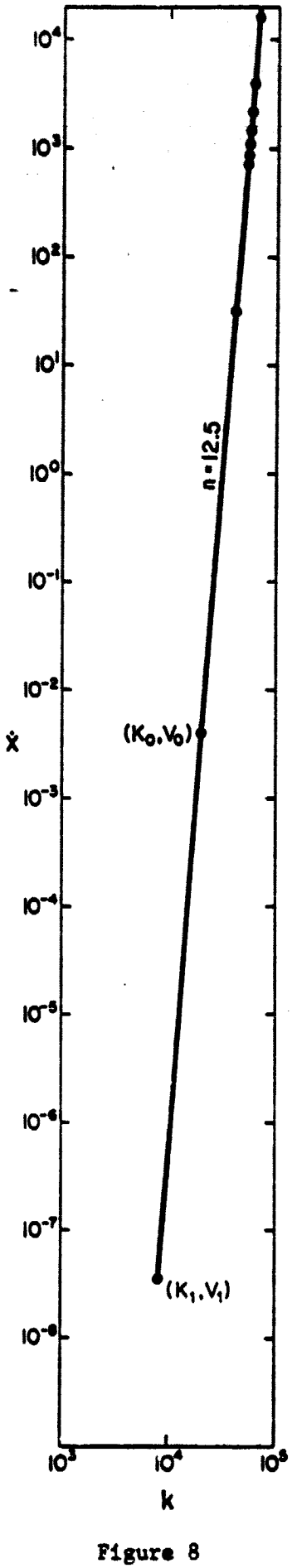
10^4
10^3
10^2
10^1
10^0
10^{-1}
10^{-2}
10^{-3}
10^{-4}
10^{-5}
10^{-6}
10^{-7}
10^{-8}
$\dot{x}$
n = 12.5
(K_0, V_0)
(K_1, V_1)
10^3
10^4
10^5
k

Figure 8

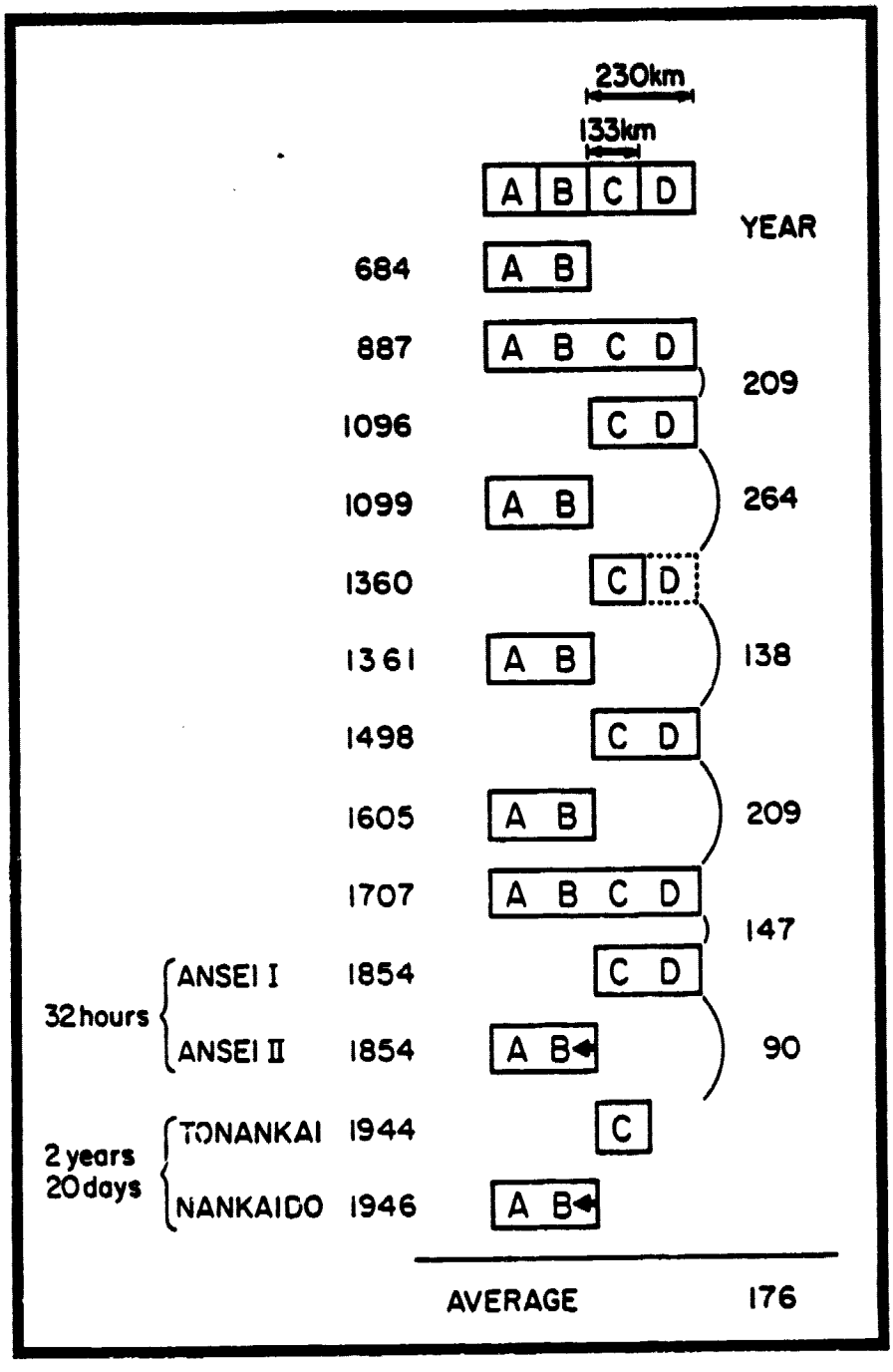
230km
133km
A B C D
YEAR
684
A B
887
A B C D
209
1096
C D
1099
A B
264
1360
C D
1361
A B
138
1498
C D
1605
A B
209
1707
A B C D
147
1854
C D
32 hours
ANSEI I
ANSEI II
1854
A B
90
2 years
20 days
TONANKAI
1944
C
NANKAIDO
1946
A B
AVERAGE
176

Figure 9

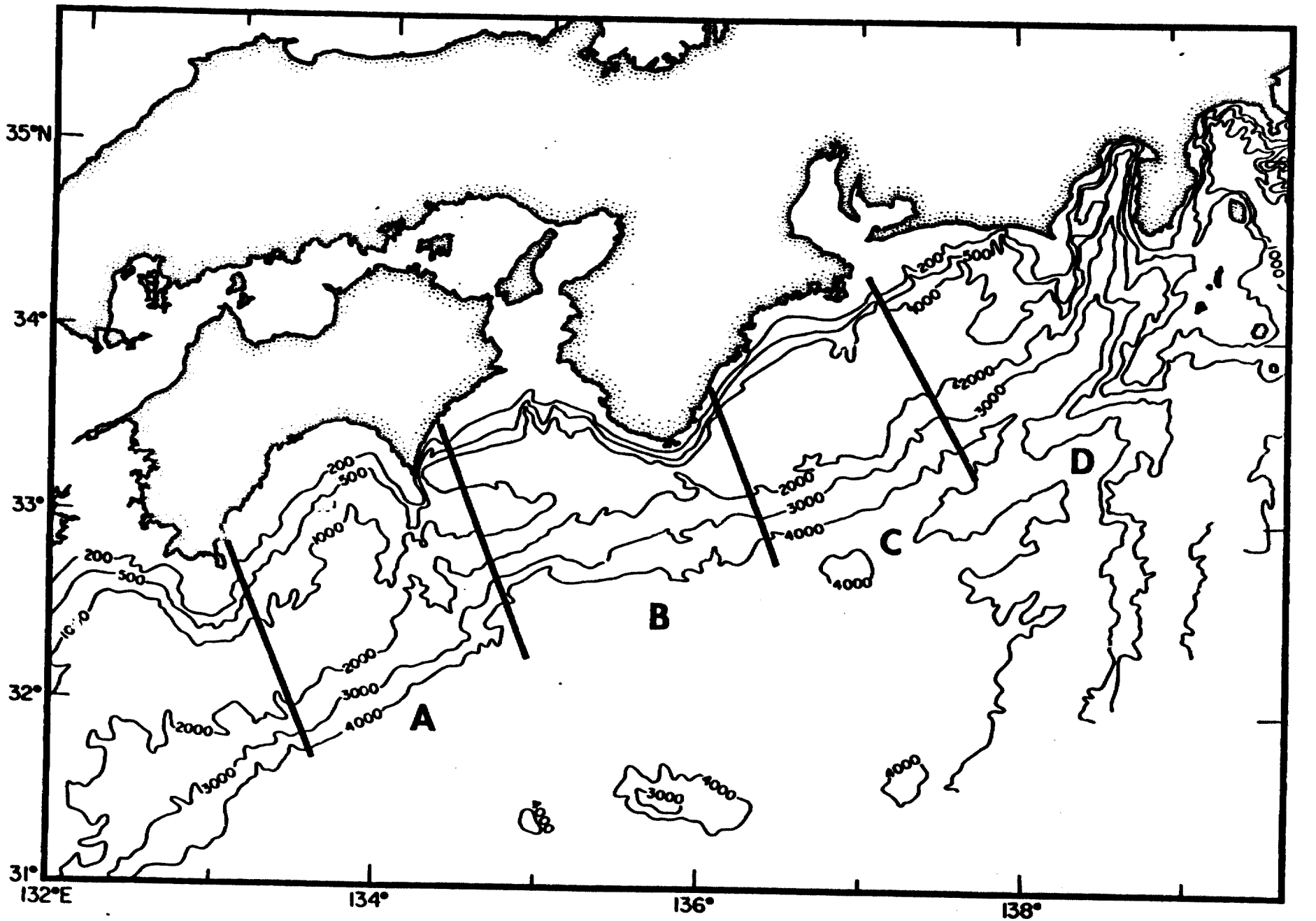
35°N
34°
33°
32°
31°
132°E
134°
136°
138°
A
B
C
D
200
300
500
1000
2000
3000
4000

Figure 10

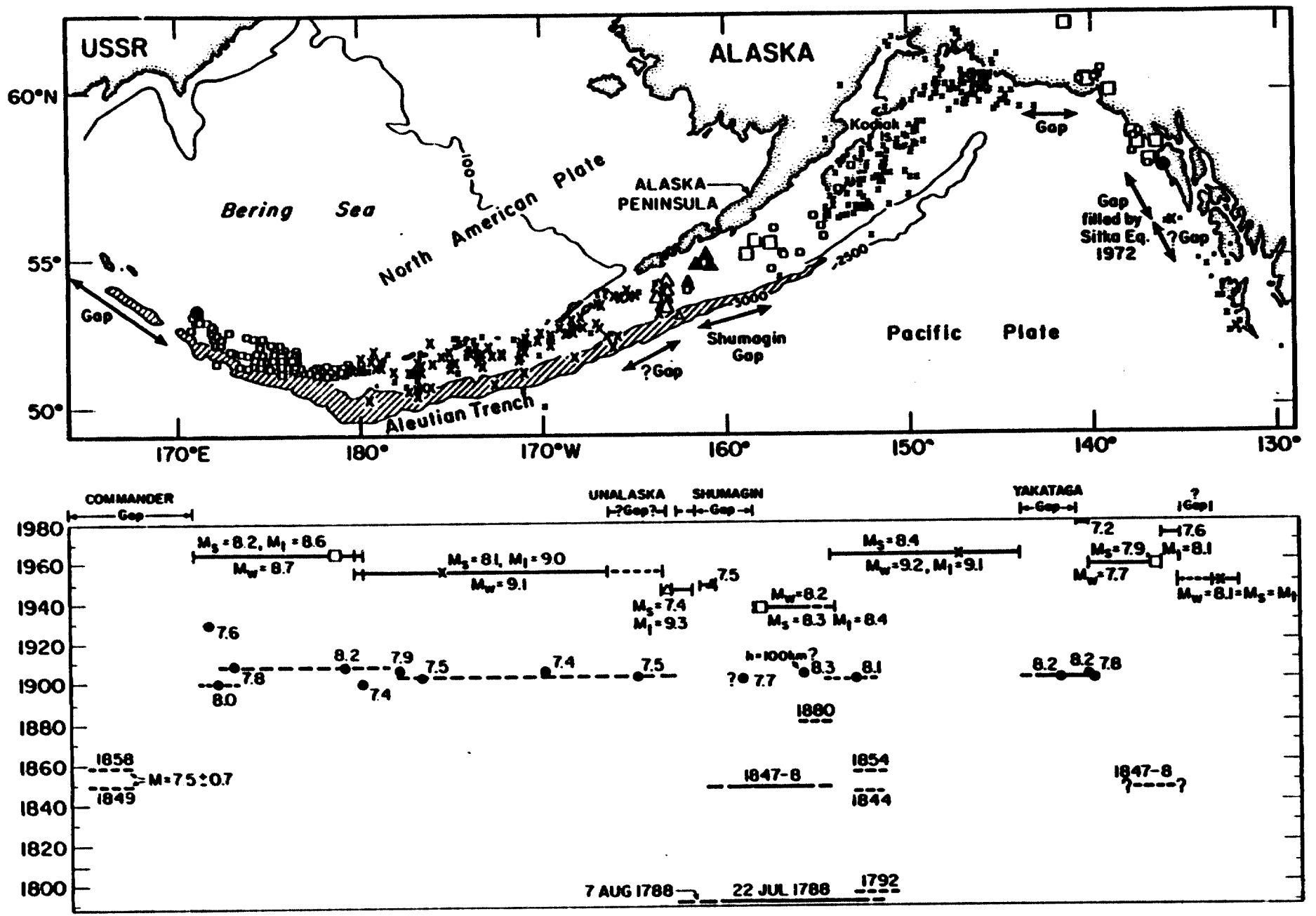
USSR
ALASKA
60°N
55°
50°
170°E
180°
170°W
160°
150°
140°
130°
Bering Sea
North American Plate
ALASKA PENINSULA
Pacific Plate
Aleutian Trench
Kodiak
Gap
Gap filled by Sitka Eq. 1972
?Gap
Shumagin Gap
?Gap
Gap
100
2000
5000
COMMANDER
Gap
UNALASKA
?Gap?
SHUMAGIN
Gap
YAKATAGA
Gap
?
Gap
1980
1960
1940
1920
1900
1880
1860
1840
1820
1800
Ms = 8.2, Ml = 8.6
Mw = 8.7
Ms = 8.1, Ml = 9.0
Mw = 9.1
Ms = 7.4
Ml = 9.3
7.5
Ms = 8.4
Mw = 9.2, Ml = 9.1
Mw = 8.2
Ms = 8.3 Ml = 8.4
7.2
7.6
Ms = 7.9
Ml = 8.1
Mw = 7.7
Mw = 8.1 = Ms = Ml
7.6
8.2
7.9
7.5
7.4
7.5
7.8
8.0
7.4
h = 100km?
?
7.7
8.3
8.1
8.2
8.2
7.8
1880
1858
1849
M = 7.5 ± 0.7
1847-8
1854
1844
1847-8
?
?
7 AUG 1788
22 JUL 1788
1792

Figure 11